Closed-Packed Colloidal Assemblies from Icosahedral Plant Virus and Polymer

Tao Li,[†] Bei Ye,[‡] Zhongwei Niu,[†] Preston Thompson,[†] Soenke Seifert,[§] Byeongdu Lee,*[,§] and Qian Wang*[,†]

Department of Chemistry and Biochemistry and Nanocenter, University of South Carolina, South Carolina 29208, Department of Nuclear, Plasma, Radiological Engineering, University of Illinois at Urbana−Champaign, Urbana, Illinois 61801, and X-ray Science Division, Advanced Photon Source, Argonne National Laboratory, 9700 South Cass Avenue, Argonne, Illinois 60439

Received October 25, 2008. Revised Manuscript Received January 9, 2009

A practical process to synthesize bio-colloidal composites was developed on the basis of the noncovalent interactions of icosahedral plant virus turnip yellow mosaic virus (TYMV) and poly(4-vinylpyridine) (P4VP). TYMV particles fully covered the surface of a P4VP ball with a hexagon-like packing. The raspberry-like morphology of TYMV-P4VP colloids and the packing pattern of TYMV were revealed by transmission electron microscopy (TEM), field-emission scanning electron microscopy (FESEM), dynamic light scattering (DLS), and synchrotron small-angle X-ray scattering (SAXS). The size of TYMV-P4VP colloids was controlled readily by varying the mass ratio of virus and polymer. A simplified model was established to explain the experimental data.

Introduction

Highly ordered structures assembled from monodispersed colloidal spheres, including organic and inorganic materials, have attracted a great deal of attention because of their potential applications such as opto-electronic devices,[1] sensors,[2] and preparing porous[3] and photonic materials.[4] Among various ordered structures, well-patterned one-dimensional (1D) and two-dimensional (2D) arrays have been extensively studied.[5,6] In addition to assemblies on solid substrates, closed-packed spherical colloids at the liquid−liquid interface, or the interface of oil emulsions in aqueous solutions, have been reported as well.[7−9] Bionanoparticles (BNPs), which include viruses and virus-like biogenic assemblies, are promising building blocks for material developments because of their monodisperse size and shape and their ability to be functionalized in a robust, well-defined manner.[10−15] Previously, through the Pickering emulsion method, icosahedral plant virus could be assembled as a monolayer at the water−perfluorodecalin interface.[16] To improve the mechanical properties of these composite structures, researchers used polymer phases instead of oil phases.[17] In this paper, we will report the fabrication of closed-packed, nanosized soft colloids through a well-controlled assembly of icosahedral virus and polymer.

Turnip yellow mosaic virus (TYMV) was used as the prototypical particle in this study. It is a spherical particle measuring ∼28 nm in diameter and can be isolated from

* Corresponding authors. E-mail: wang@mail.chem.sc.edu(Q.W.); blee@aps.anl.gov(B.L.)
[†] University of South Carolina.
[‡] University of Illinois at Urbana–Champaign.
[§] Argonne National Laboratory.

(1) (a) Tessier, P. M.; Velev, O. D.; Kalambur, A. T.; Lenhoff, A. M.; Rabolt, J. F.; Kaler, E. W. *Adv. Mater.* **2001**, *13*, 396. (b) Yang, P.; Wirnsberger, G.; Huang, H. C.; Cordero, S. R.; McGehee, M. D.; Scott, B.; Deng, T.; Whitesides, G. M.; Chmelka, B. F.; Buratto, S. K.; Stucky, G. D. *Science* **1998**, *282*, 1111. (c) Xia, Y.; Gates, B.; Yin, Y.; Lu, Y. *Adv. Mater.* **2001**, *13*, 396. (d) Sirringhaus, H.; Tessler, N.; Friend, R. H. *Science* **1998**, *280*, 1741.

(2) (a) Haes, A. J.; Hall, W. P.; Chang, L.; Klein, W. L.; Van Duyne, R. P. *Nano Lett.* **2004**, *4*, 1029. (b) Valsesia, A.; Colpo, P.; Silvan, M. M.; Meziani, T.; Geccone, G.; Rossi, F. *Nano Lett.* **2004**, *4*, 1047. (c) Andersson, H.; Vander Wijngaart, W.; Stemme, G. *Electrophoresis* **2001**, *22*, 249. (d) Hagleitner, C.; Hierlemann, A.; Lange, D.; Kummer, A.; Kerness, N.; Brand, O.; Baltes, H. *Nature* **2001**, *414*, 293. (e) Holtz, J. H.; Asher, S. A. *Nature* **1997**, *389*, 829.

(3) (a) Velev, O. D.; Tessier, P. M.; Lenhoff, A. M.; Kaler, E. W. *Nature* **1999**, *401*, 548. (b) Jiang, P.; Hwang, K. S.; Mileman, D. M.; Bertone, J. F.; Colvin, V. L. *J. Am. Chem. Soc.* **1999**, *121*, 11630. (c) Park, S. H.; Xia, Y. *Adv. Mater.* **1998**, *10*, 1045. (d) Yin, J.; Wang, Z. L. *Adv. Mater.* **1998**, *11*, 469. (e) Lu, Z.-X.; Namboodiri, A.; Collinson, M. M. *ACS Nano* **2008**, *2*, 993.

(4) (a) Dinsmore, A. D.; Crocker, J. C.; Yodh, A. G. *Curr. Opin. Colloid Interface Sci.* **1998**, *3*, 5. (b) Xia, Y.; Gates, B.; Yin, Y.; Lu, Y. *Adv. Mater.* **2000**, *12*, 693. (c) Holtz, J. H.; Asher, S. A. *Nature* **1997**, *389*, 829. (d) Gates, B.; Xia, Y. *Adv. Mater.* **2000**, *12*, 1329. (e) Yang, S. M.; Ozin, G. M. *Chem. Commun.* **2000**, 2057. (f) Wang, D.; Caruso, F. *Adv. Mater.* **2001**, *13*, 350. (g) Wang, Y.; Ibisate, M.; Li, Z.; Xia, Y. *Adv. Mater.* **2006**, *18*, 471.

(5) (a) Yin, Y.; Xia, Y. *Adv. Mater.* **2001**, *13*, 267. (b) Lu, Y.; Yin, Y.; Xia, Y. *Adv. Mater.* **2001**, *13*, 34. (c) Yin, Y.; Lu, Y.; Xia, Y. *J. Am. Chem. Soc.* **2001**, *123*, 771. (d) Yin, Y.; Lu, Y.; Gates, B.; Xia, Y. *J. Am. Chem. Soc.* **2001**, *123*, 8718. (e) Chol, D. G.; Jang, S. G.; Yu, H. K.; Yang, S. M. *Chem. Mater.* **2004**, *16*, 3410. (f) Lee, I.; Zheng, H.; Rubner, M. F.; Hammond, P. T. *Adv. Mater.* **2002**, *14*, 573. (g) Choi, W. M.; Park, O. O. *Nanotechnology* **2006**, *17*, 325. (h) Zheng, H.; Lee, I.; Rubner, M. F.; Hammond, P. T. *Adv. Mater.* **2002**, *14*, 569.

(6) (a) Cong, H.; Cao, W. *Langmuir* **2003**, *19*, 8177. (b) Griesebock, B.; Egen, M.; Zental, R. *Chem. Mater.* **2002**, *14*, 4023. (c) Cui, J.; Kretzschmar, I. *Langmuir* **2006**, *22*, 8281. (d) Zhang, G.; Wang, D.; Gu, Z.; Hartmann, J.; Möhwald, H. *Chem. Mater.* **2005**, *17*, 5268. (e) Zhang, G.; Wang, D.; Möhwald, H. *Chem. Mater.* **2006**, *18*, 3985. (f) Varghese, B.; Chiong, F. C.; Sindhua, S.; Yu, T.; Lim, C. T.; Valiyaveettil, S.; Sow, C. H. *Langmuir* **2006**, *22*, 8248. (g) Sun, F.; Yu, J. C.; Wang, X. *Chem. Mater.* **2006**, *18*, 3774.

(7) (a) Lin, Y.; Skaff, H.; Böker, A.; Dinsmore, A. D.; Emrick, T.; Russell, T. P. *J. Am. Chem. Soc.* **2003**, *125*, 12690. (b) Skaff, H.; Lin, Y.; Tangirala, R.; Breitenkamp, K.; Böker, A.; Russell, T. P.; Emrick, T. *Adv. Mater.* **2005**, *17*, 2082. (c) Böker, A.; He, J.; Emrick, T.; Russell, T. P. *Soft Matter* **2007**, *3*, 1231.

(8) Chen, T.; Colver, P. J.; Bon, S. A. F. *Adv. Mater.* **2007**, *19*, 2286.

(9) Dinsmore, A. D.; Hsu, M. F.; Nikolaides, M. G.; Marquez, M.; Bausch, A. R.; Weitz, D. A. *Science* **2002**, *298*, 1006.

10.1021/cm802922z CCC: $40.75
Published on Web 02/23/2009

infected plants in gram quantities by a convenient procedure.[18] Compared with other plant viruses, TYMV has unique advantages to be used in chemistry, biomedical applications, and material developments. First, empty TYMV capsids, which can be isolated naturally or generated artificially,[19] are good templates to introduce useful materials such as quantum dots or drugs. Second, TYMV particles are more stable at various conditions such as a wide temperature range from 4 °C to room temperature for months, a wide pH range from 4 to 10, and a variety of organic solvents. Meanwhile, TYMV has shown to be a robust platform for its conjugation with different molecules and has been used as a scaffold for the sensor development with a time-resolved fluoroimmuno assay.[12a,20] Recently, TYMV has been used as an exemplary bionanoparticle to modulate the osteogenesis of the bone marrow stromal cells.[21] Here we reported a practical process to synthesize biocolloidal composites based on the noncovalent interactions of TYMV and poly(4-vinylpyridine) (P4VP).

Experimental Section

Materials. P4VP and dimethylformamide (DMF) were purchased from Sigma-Aldrich and used as received. Water (18.2 MΩ) was obtained from a Milli-Q system (Millipore). TYMV was isolated from the infected Chinese cabbage as reported.[20]

Typical Procedure to Synthesize TYMV-P4VP. A solution of P4VP (M_w 60 000 Da) in DMF (2.0 mg mL^{-1}, 0.5 mL) was slowly added to a TYMV solution with different amounts of 0.1, 0.2, and 0.3 mg in pure water while stirring. The final concentration of P4VP was 0.006 mg mL^{-1}, and the volume percentage of DMF was ~3%. Then the samples were dialyzed against water (2 × 1 L) with M_W 3500 cutoff dialysis tubing (Pierce) to remove the DMF at room temperature for 48 h.

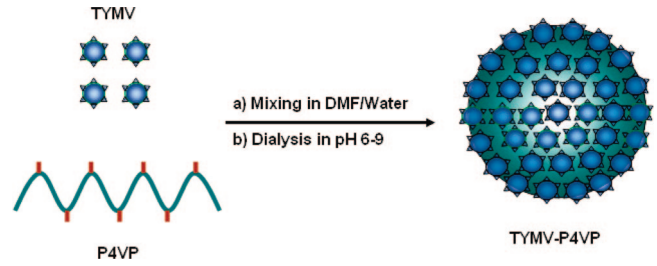

Figure 1. Schematic illustration of the formation of TYMV-P4VP raspberry-like colloids.

Analysis. Transmission electron microscopy (TEM) analysis was carried out by depositing 20 μL aliquots of each sample onto 100-mesh carbon coated copper grids for 2 min. The grids were then stained with 20 μL of uranyl acetate and imaged with a Hitachi H-8000 electron microscope. For field-emission scanning electron microscopy (FESEM) analysis, the samples were dried overnight and coated with Pt and then observed by a Hitachi S4800 electron microscope. The dynamic light scattering (DLS) analysis was performed by a submicrometer particle sizer AutodillutePAT model 370. The synchrotron small-angle X-ray scattering (SAXS) was performed at Sector 12, Advanced Photon Source in Argonne National Laboratory; a 12 keV X-ray beam and a flow cell equipped with 2 mm thick quartz capillary were used.

Results and Discussion

Figure 1 shows a general pathway to generate the hybridized composite colloids (TYMV-P4VP) by mixing TYMV with P4VP at neutral pH. P4VP was selected because of its well-established assembly properties with nanoparticles (or other polymers) presumably through hydrogen bonding.[22,23] In the first experiment, a solution of P4VP (M_w 60 000 Da, 1 mg in 0.5 mL DMF) was slowly added to a solution of TYMV (0.2 mg in 16.5 mL pure water) with vigorous stirring. The final product was dialyzed against pure water. The final product was characterized using TEM, FESEM and DLS (Figure 2). Stable particles could be observed using TEM after the product was negatively stained with uranyl acetate (images a and b in Figure 2). As shown by FESEM image (Figure 2d), the final product consists of spherical colloids and TYMV particles cover the entire exterior surface of P4VP balls homogeneously. The TYMV appears to be closed-packed on the colloidal ball with a raspberry-like morphology. The hydrodynamic diameter of the TYMV-P4VP colloidal assemblies is in the range of 365 ± 160 nm as measured by DLS (Figure 2c). When P4VP was added into pure water without TYMV, P4VP was mostly precipitated after the removal of DMF due to the low solubility in water. Clearly, TYMV served as a surfactant-like agent that

(10) (a) Wang, Q.; Lin, T.; Tang, L.; Johnson, J. E.; Finn, M. G. *Angew. Chem., Int. Ed.* **2002**, *41*, 459. (b) Wang, Q.; Kaltgrad, E.; Lin, T.; Johnson, J. E.; Finn, M. G. *Chem. Biol.* **2002**, *9*, 805. (c) Wang, Q.; Chan, T. R.; Hilgraf, R.; Fokin, V. V.; Sharpless, K. B.; Finn, M. G. *J. Am. Chem. Soc.* **2003**, *125*, 3192. (d) Raja, K. S.; Wang, Q.; Gonzalez, M. J.; Manchester, M.; Johnson, J. E.; Finn, M. G. *Biomacromolecules* **2003**, *4*, 472. (e) Wang, Q.; Lin, T.; Johnson, J. E.; Finn, M. G. *Chem. Biol.* **2002**, *9*, 813. (f) Wang, Q.; Raja, K. S.; Janda, K. D.; Lin, T.; Finn, M. G. *Bioconjugate Chem.* **2003**, *14*, 38.
(11) (a) Schlick, T.; Ding, Z.; Kovacs, E.; Francis, M. *J. Am. Chem. Soc.* **2005**, *127*, 3718. (b) Holder, P. G.; Francis, M. *Angew. Chem., Int. Ed.* **2007**, *46*, 4370.
(12) (a) Barnhill, H. N.; Gillet, S.; Ziessel, R.; Charbonnière, L. J.; Wang, Q. *J. Am. Chem. Soc.* **2007**, *129*, 7799. (b) Zeng, Q.; Li, T.; Cash, B.; Li, S.; Xie, F.; Wang, Q. *Chem. Commun.* **2007**, 1453. (c) Lee, L. A.; Wang, Q. *Nanomedicine* **2006**, *2*, 137. (d) Lin, Y.; Böker, A.; He, J.; Kevin, S.; Xiang, H.; Abetz, C.; Li, X.; Wang, J.; Emrick, T.; Long, S.; Wang, Q.; Balazs, A.; Russell, T. P. *Nature* **2005**, *434*, 55.
(13) (a) Douglas, T.; Yong, M. *Nature* **1998**, *393*, 152. (b) Douglas, T.; Yong, M. *Adv. Mater.* **1999**, *11*, 679. (c) Douglas, T.; Yong, M. *Science* **2006**, *312*, 873.
(14) (a) Blum, A. S.; Soto, C. M.; Wilson, C. D.; Cole, J. D.; Kim, M.; Gnade, B.; Chatterji, A.; Ochoa, W. F.; Lin, T.; Johnson, J. E.; Ratna, B. R. *Nano Lett.* **2004**, *4*, 867. (b) Blum, A. S.; Soto, C. M.; Wilson, C. D.; Brower, T. L.; Pollack, S. K.; Schull, T. L.; Chatterji, A.; Lin, T.; Johnson, J. E.; Amsinck, C.; Franzon, P.; Shashidhar, R.; Ratna, B. R. *Small* **2005**, *1*, 702. (c) Cheung, C. L.; Chung, S. W.; Chatterji, A.; Lin, T. W.; Johnson, J. E.; Hok, S.; Perkins, J.; De Yoreo, J. J. *J. Am. Chem. Soc.* **2006**, *128*, 10801.
(15) (a) Lee, S. W.; Mao, C.; Flynn, C. E.; Belcher, A. M. *Science* **2002**, *296*, 892. (b) Nam, K. T.; Kim, D. W.; Yoo, P. J.; Chiang, C. Y.; Meethong, N.; Hammond, P. T.; Chiang, Y. M.; Belcher, A. M. *Science* **2006**, *312*, 885. (c) Chiang, C. Y.; Mello, C. M.; Gu, J.; Silva, E. C. C. M.; Van Vliet, K. J.; Belcher, A. M. *Adv. Mater.* **2007**, *19*, 826.
(16) Russell, J. T.; Lin, Y.; Böker, A.; Long, S.; Carl, P.; Zettl, H.; He, J.; Sill, K.; Tangirala, R.; Emrick, T.; Littrell, K.; Thiyagarajan, P.; Cookson, D.; Fery, A.; Wang, Q.; Russell, T. P. *Angew. Chem., Int. Ed.* **2005**, *44*, 2420.
(17) Li, T.; Niu, Z.; Emrick, T.; Russell, T. P.; Wang, Q. *Small* **2008**, *4*, 1624.
(18) Klug, A.; Finch, J. T.; Franklin, R. E. *Nature* **1957**, *179*, 683.
(19) Canady, M. A.; Larson, S. B.; Day, J.; McPherson, A. *Nat. Struct. Biol.* **1996**, *3*, 771.
(20) Barnhill, H. N.; Reuther, R.; Ferguson, P. L.; Dreher, T.; Wang, Q. *Bioconjugate Chem.* **2007**, *18*, 852.
(21) Kaur, G.; Valarmathi, M. T.; Potts, J. D.; Wang, Q. *Biomaterials* **2008**, *29*, 4074.
(22) (a) Chen, D. Y.; Jiang, M. *Acc. Chem. Res.* **2005**, *38*, 494. (b) Zhang, Y. W.; Jiang, M.; Zhao, J. X.; Ren, X. W.; Chen, D. Y.; Zhang, G. Z. *Adv. Funct. Mater.* **2005**, *15*, 695. (c) Liu, X. K.; Jiang, M. *Angew. Chem., Int. Ed.* **2006**, *45*, 3846.
(23) (a) Du, H.; Zhu, J.; Jiang, W. *J. Phys. Chem. B* **2007**, *111*, 1938. (b) Zhu, J.; Yu, H.; Jiang, W. *Macromolecules* **2005**, *38*, 7492.

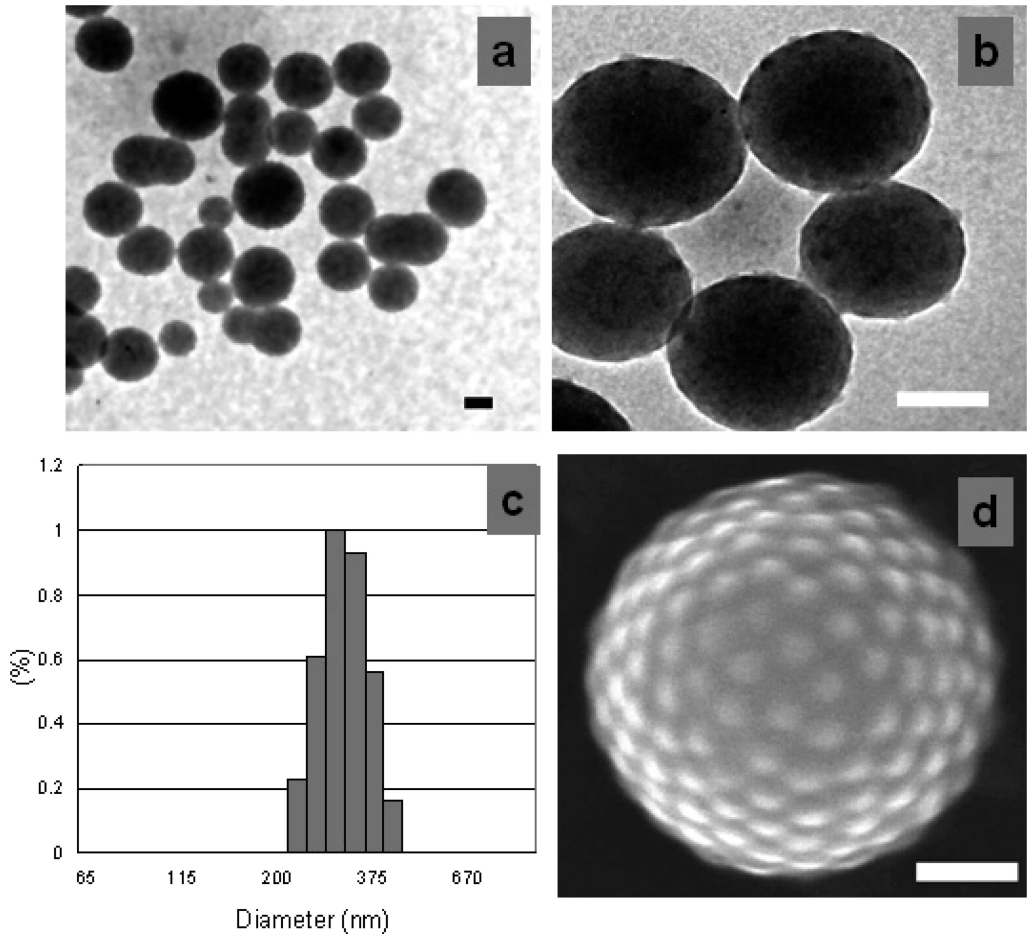

Figure 2. (a, b) TEM, (c) DLS, and (d) FESEM analysis of TYMV-P4VP. The mass ratio of TYMV and P4VP was 0.2. All scale bars are 100 nm.

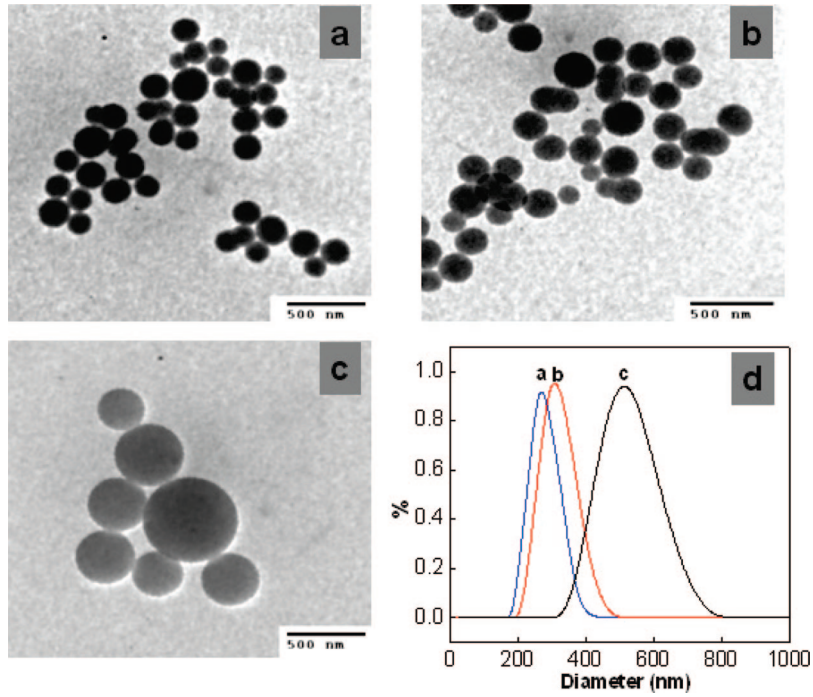

Figure 3. (a−c) TEM images and (d) DLS analysis of TYMV-P4VP with different M_{TYMV}/M_{P4VP} ratios: (a) 0.3, (b) 0.2, and (c) 0.1.

stabilized hydrophobic P4VP colloids. The size difference of TYMV-P4VP composites observed from DLS and EM techniques was more likely attributed to different states of the investigated samples. FESEM and TEM images were taken from dry samples, whereas DLS was applied to the solution of final composites.

TEM images and DLS results of TYMV-P4VP colloids prepared with varying the mass ratios of TYMV and P4VP

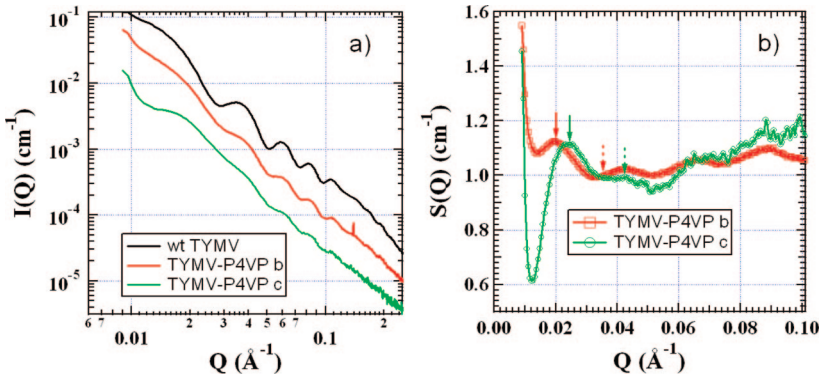

Figure 4. (a) SAXS data of wt-TYMV and TYMV-P4VP **b** and **c**. (b) Structural factor S(Q) of TYMV-P4VP **b** and **c**.

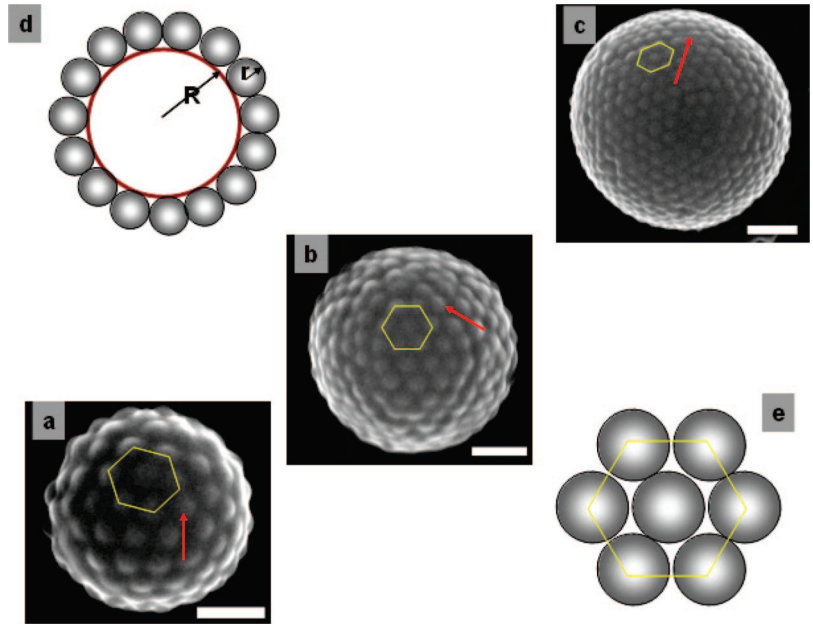

Figure 5. (a−c) Representative FESEM images of TYMV-P4VP of samples **a**, **b**, and **c** (the arrows point to the packing defect). All scale bars are 100 nm. (d) Cross-sectional view of schematic model of TYMV-P4VP composite, where *R* and *r* are the radii of P4VP ball and TYMV, respectively. (e) A schematic model of hexagonally packed TYMV particles on the surface of the P4VP ball.

(M_{TYMV}/M_{P4VP}) are presented in Figure 3. The average hydrodynamic diameters of three samples designated as **a**, **b**, and **c**, of which M_{TYMV}/M_{P4VP} ratios were 0.3, 0.2, and 0.1, respectively, were 275, 365, and 548 nm. Consistent to the DLS result, TEM (Figure 3(a-c)) and FESEM (Figure 5) also suggested that the sizes of TYMV-P4VP colloids increased as the mass ratios of TYMV to P4VP decreased. Interestingly, colloids were fully covered with TYMV particles in all three samples as shown by FESEM (Figure 5). This explains why the sizes of colloids were bigger as larger ratio of P4VP was added into a TYMV solution (see later the mathematical model).

To understand the interactions between TYMV and P4VP, we performed synchrotron SAXS to analyze the TYMV-P4VP colloids. SAXS has been successfully used to visualize polymers tethered on tobacco mosaic virus in our previous work.[24] When TYMV particles are closed-packed, the diffraction peak associated with the packing structure of TYMV will appear on SAXS curves, and the peak will be sharper as the packing structure possesses a longer range ordering. When TYMV particles are closed-packed to form a hexagonal structure on a flat surface, they will generate an interparticle distance peak at $Q = Q^* = 4\pi/\sqrt{3}D$, which is around 0.02 Å^{-1} in this case. Q^* denotes the peak position of the first order diffraction peak, and D is the nearest neighbor distance, which equals to the diameter of TYMV for a perfect close packing. In our study, the peak was not observed on SAXS curves of wtTYMV in aqueous solutions (Figure 4a), indicating that TYMV did not form aggregates without P4VP. However the peak was more distinctive or sharper on sample **c** (Figure 4a). For clarity, structure factors $S(Q)$ of TYMV-P4VP samples **b** (red square) and **c** (green circle) were calculated from the SAXS data in Figure 4a and plotted in Figure 4b. Note that broad peaklike feature at $Q \approx 0.04$, 0.065, 0.09 Å^{-1} and other higher Q are not diffraction peaks but are caused by dampening of the form factor oscillation of TYMV due to a loss of the scattering contrast (density difference between P4VP and TYMV is smaller than that between water and TYMV).

(24) (a) Niu, Z.; Bruckman, M. A.; Kotakadi, V. S.; He, J.; Emrick, T.; Russell, T. P.; Yang, L.; Wang, Q. *Chem. Commun.* **2006**, 3019. (b) Niu, Z.; Bruckman, M. A.; Li, S.; Lee, L. A.; Lee, B.; Pingali, S. V.; Thiyagarajan, P. *Langmuir* **2007**, *23*, 6719.

First-order diffraction peaks observed were denoted with solid arrows in Figure 4b. It was not difficult to see different Q^* positions for TYMV-P4VP **b** and **c**, where Q^* of TYMV-P4VP **c** appeared a higher Q. When nearest neighbor distance D was calculated using Bragg relation $D = 2\pi/Q^*$ assuming random arrangement of TYMV on P4VP ball without any symmetry, D would then be 31 and 26 nm for samples **b** and **c**, respectively. The value for sample **c**, however, was not acceptable because the diameter of TYMV obtained by fitting the form factor in Figure 4a turned out to be 30 nm, suggesting that D must be equal to or larger than 30 nm. This result indicated that the packing structure of TYMV had a higher symmetry rather than a random arrangement. The higher symmetric packing was most likely a hexagonal arrangement as was observed from FESEM images in Figure 5. With assuming hexagonal symmetry, D values for sample **b** and **c** were calculated as 36 and 30 nm, respectively. Solid and broken arrows in Figure 4b depicted positions of the first and second order diffraction peaks in case of 2D hexagonal packing, which located at $Q/Q^* = 1$ and $\sqrt{3}$, respectively. Although $S(Q)$ of sample **b** does not present the second-order diffraction peak, sample **c** does. On the basis of this symmetry information, D values for samples **b** and **c** could be concluded as 31 and 30 nm, respectively. Thus, it was clear that TYMVs on both samples were closed-packed and degree of packing was better for sample **c**.

A perfect hexagonally closed-packed complex will yield a planar structure instead of a spherical shell of a 3D ball. Therefore, to obtain a quasi-spherical coverage, defects are necessary. There should be more defects as the curvature of the ball is smaller. Distribution of defect points probably prevents a long-range ordering of TYMV and causes diffraction peaks get broader. In fact, defects in TYMV arrangement on P4VP, i.e., not-perfect hexagonal patterns, were easily observed on FESEM images (see hexagonal lattices in Figure 5a−c and e) especially predominantly at smaller size of TYMV-P4VP colloids, which was also consistent with our SAXS results: sample **c** having the largest curvature among our samples presented hexagonal arrangement, whereas sample **b** did not.

Sizes of TYMV-P4VP balls with different mass ratios of TYMV and P4VP can be roughly estimated with a simple model. Our model is a simplified geometric one similar to the simulation of core−shell structure in literatures.[8] Followings are assumed for simplicity: (a) P4VP ball is fully covered with TYMV; (b) there is no free TYMV particle in solution; (c) both TYMV and TYMV-P4VP are monodisperse; (d) TYMVs are hexagonally packed on the surface.

The expressions for the number of TYMV (Ns) are obtained from both mass (eq 1) and coverage (eq 2)

$$N_s = \frac{m_s N_A}{M_w} \tag{1}$$

$$N_s = nN_b = \frac{A_b}{A_s}\frac{m_b}{\rho V} = \frac{4\pi R^2}{2\sqrt{3}r^2}\frac{3/4m_b}{\rho\pi R^3} = \frac{\sqrt{3}/2m_b}{r^2\rho R} \tag{2}$$

where n is the number of TYMVs on a P4VP ball; N_s and N_b are the numbers of TYMVs and P4VP balls, respectively; m_s and m_b are their total weights, respectively; r and R are the radii of TYMV and P4VP ball, respectively; ρ is the density of P4VP ball; A_s is the area of the surface covered by TYMV particles; A_b is the surface area that P4VP ball can provide; N_A is Avogadro's number; M_w is the molecular weight of TYMV; V is the volume of P4VP ball. From eq 1 and 2

$$R = \frac{\sqrt{3}/2m_b M_w}{r^2\rho m_s N_A} \tag{3}$$

According to eq 3, R is proportional to the ratio of m_b/m_s, as is observed in our experiment. Taking into account $\rho = 0.984$ g/mL $= 0.984 \times 10^{-21}$ g/nm^3, $r = 15$ nm, $M_w = 5.5 \times 10^6$ g/mol, and $N_A = 6.022 \times 10^{23}$/mol, R values were approximately 119, 179, and 357 nm for the ratio m_s/m_b of 0.3, 0.2, and 0.1, respectively. The final TYMV-P4VP diameters ($d = 2R + 4r$) were then 298, 418, and 774 nm for sample **a**, **b**, and **c**, respectively. Considering the large polydispersity of the colloids, the estimated values agree very well with the experimental data 275 ± 32, 365 ± 160, and 548 ± 184 nm for samples **a**, **b**, and **c**.

It should be noticed that the assembly process could be performed either in pure water or in buffer solutions. The final TYMV-P4VP colloids were very stable, which could maintain the original morphology for weeks at room temperature. Additionally, the assembly processes are reversible and can be controlled by varying the solution pH values. At pH 5 to 8, the pyridine groups of P4VP maintain unprotonated form, and P4VP is fairly hydrophobic; therefore, the TYMV-P4VP colloids could be readily produced. However, at lower pH (3−4), the core−shell structures would dissociate and TYMV could be recovered.

Conclusions

In summary, a facile strategy to fabricate bio-colloidal composites has been developed thorough the self-assembly of TYMV and P4VP. The final assembly forms raspberry-like morphology. The closed-packed hexagonal arrangement of TYMV particles on P4VP colloids was proved by FESEM and SAXS analysis. During the assembly process, virus behaves as a surfactant-like agent to stabilize the P4VP ball. The size of the colloids can be readily tailored by varying the mass ratios of TYMV and P4VP. Larger colloidal particles can be obtained when smaller mass ratio of virus to polymer is used. Such colloids may find applications as carriers for drug release systems if other targeting proteins (like monoclonal antibodies) are used in place of TYMV, which is undergoing in our laboratory. Furthermore, this method may open a new way to assemble other spherical particles on the surface of polymeric colloids.

Acknowledgment. We are grateful for the support from the NSF, the Alfred P. Sloan Scholarship, the Camille Dreyfus Teacher Scholar Award, DoD-BCRP, and the W. M. Keck Foundation. We are also thankful for Dr. C. Stork for the help on the DLS characterization and Drs. J. S. Hudson and D. Cash for the help on the FESEM analysis at Clemson University.

CM802922Z